Liquid Crystals
Publication details, including instructions for authors and subscription information:
http://www.informaworld.com/smpp/title~content=t713926090

Dual nature of a tin-containing liquid crystalline side group homopolymer

H. Kresse[a]; J. Lindau[a]; J. Salfetnikova[a]; D. Reichert[b]; O. Pascui[b]; E. Hempel[b]
[a] Martin-Luther-Universität Halle, Institut für Physikalische Chemie, Mühlpforte 1, D-06108 Halle, Germany [b] Martin-Luther-Universität Halle, FB Physik, D-06108 Halle, Germany

To cite this Article Kresse, H. , Lindau, J. , Salfetnikova, J. , Reichert, D. , Pascui, O. and Hempel, E.(2005) 'Dual nature of a tin-containing liquid crystalline side group homopolymer', Liquid Crystals, 32: 2, 213 — 219
To link to this Article: DOI: 10.1080/02678290412331327983
URL: http://dx.doi.org/10.1080/02678290412331327983

Liquid Crystals, Vol. 32, No. 2, February 2005, 213–219

Dual nature of a tin-containing liquid crystalline side group homopolymer

H. KRESSE*†, J. LINDAU†, J. SALFETNIKOVA†, D. REICHERT‡, O. PASCUI‡ and E. HEMPEL‡

†Martin-Luther-Universität Halle, Institut für Physikalische Chemie, Mühlpforte 1, D-06108 Halle, Germany
‡Martin-Luther-Universität Halle, FB Physik, Friedemann-Bach-Platz 6, D-06108 Halle, Germany

(*Received 17 January 2003; in final form 14 July 2004; accepted 15 September 2004*)

Two tin-containing homopolymers, one liquid crystalline and the other non-mesomorphic, were synthesized and characterized by different relaxation methods (dielectric, calorimetric, NMR). The results prove the existence of two glass transition temperatures related to the dynamics of the main chain and of the liquid crystalline side group, respectively. The reason for this effect is based on a phase separation on nanometer scale.

1. Introduction

Phase segregation is a classical principle for a systematic 'construction' of liquid crystalline materials [1, 2]. On one hand, such a segregation can take place at the molecular level, such as, for example, in amphiphilic molecules organized in bilayers, micelles and in more complicated structures [3]. On the other hand, much larger units may be organized in block copolymers with the formation of super-structures made of non-compatible blocks [4, 5]. In the latter case, for example, two glass transition temperatures related to the two different blocks of the polymer are detected [6]. The presence of two glass transitions in one system gives direct evidence for a separation into two phases.

However one could expect a type of phase separation also to occur in side chain LC homopolymers in which the main chains and side groups are ordered in different ways, thus forming LC and liquid-like phases; this has been demonstrated by X-ray analysis for side chain homopolymers containing either Sn or Si–O groups in the backbone [7–10]. However no confirmation of this was obtained by dynamic measurements. At the same time the presence of two phases was demonstrated in amorphous poly(*n*-alkyl methacrylates) by both X-ray and dynamics methods, including enthalpy relaxation measurements [11–13]. These data show the importance of combined structural and dynamical approaches for the study of glass transition processes [14].

Recently we have synthesized tin-containing side group polymers with a strong $-NO_2$ dipole in the terminal position of the mesogenic fragment. It is worth noting that the tin-containing part and the mesogenic fragment are miscible. The tin atoms were introduced into the main chain in order to make this part more visible with X-rays. This polymer has a liquid crystalline SmC structure although the main chain is reported to be statistically distributed [7].

The major objective of this paper is to analyse the dynamic behavior of a tin-containing polymer in order to obtain independent evidence for phase separation in such homopolymers. Among the techniques used in this research the dielectric method plays an important role. It allows us to distinguish the relaxation processes occurring with respect to the chemical structure of a polymer molecule and in particular its polar parts [15].

2. Samples and phase behaviour

The polymers studied are:

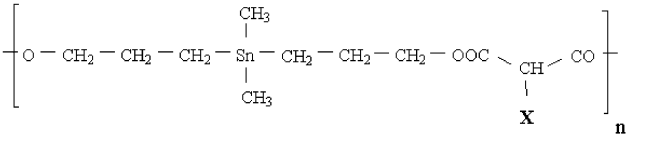

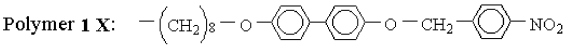

Polymer **2** X: $-C_2H_5$

Polymer **1** was chosen for practical considerations involving the dynamic measurements because its chemical structure allows us to avoid a crossover of phase and glass transitions and to measure more precisely the dynamical effects. To compare the LC polymer behaviour with that of an amorphous one, polymer **2**

*Corresponding author. Email: kresse@chemie.uni-halle.de

Liquid Crystals
ISSN 0267-8292 print/ISSN 1366-5855 online © 2005 Taylor & Francis Group Ltd
http://www.tandf.co.uk/journals
DOI: 10.1080/02678290412331327983

was chosen as a control sample. Both homopolymers were synthesized according to the route described in [7].

Polymer **1**, containing a side chain LC fragment, is characterized by GPC to have a polycondensation degree $n_1=29$. The polymorphism I 396 SmA with two steps in c_p at about 348 and 290 K is detected by polarization microscopy and standard DSC, using a cooling rate of 10 K min^{-1}. Only one glass transition at about 203 K is found for polymer **2**, containing the ethyl side group ($n_2=28$) which is seen as a c_p-step in the DSC trace.

3. Dielectric experiments

Dielectric measurements were performed using a Solartron–Schlumberger impedance analyser in a glass cell coated with gold ($d=0.005$ cm). Temperature regulation was achieved by a Eurotherm 905S. Experimental data of polymer **1** at two temperatures are shown in figure 1. One can easily identify three relaxation ranges denoted by 1–3, beginning from the lowest frequency. The first is apparent only in the dispersion curve while the third has to be separated from the standing wave in the equipment and is more visible at lower temperatures.

The data were analysed using the following equation for the complex dielectric function $\varepsilon^*(\omega)=\varepsilon'(\omega)-i\varepsilon''(\omega)$:

$$\varepsilon^*(\omega)=\varepsilon_2+\frac{\varepsilon_0-\varepsilon_1}{1+(i\omega\tau_1)^{1-\alpha_1}}+\frac{\varepsilon_1-\varepsilon_2}{1+(i\omega\tau_2)^{1-\alpha_2}}-\frac{iA}{f^M}+\frac{B}{f^N} \quad (1)$$

Here ε_i are the limits of the dielectric function, $\omega=2\pi f$ (f=frequency), τ=relaxation times, α=Cole–cole distribution parameters while A, M, B and N are fitting parameters to compensate for the conductivity and capacity of the double layer.

The obtained limits of the dielectric functions ε_i and the related relaxation times τ_i are presented in the figures 2 and 3, respectively. The high dielectric increment of the low frequency mechanism $\varepsilon_0-\varepsilon_1$ indicates that the related relaxation time τ_1 is associated with the dynamics of the strong polar NO_2 fragment in the side group [15] (δ-relaxation) while the second process is commonly considered as dynamics of the main chain (α-relaxation) [16]). The less intense third process, which is superimposed at high frequencies by the standing wave in the equipment, shows a very strong temperature dependence. This means that the dielectric process related to this mode cannot correspond to a local process associated with the dynamics of a small group. Therefore we assume that it is caused by the reorientation of the whole side group about the long axes [17]. This assignment is confirmed in § 5 by NMR investigations. In contrast to the behaviour of polymer **1**, polymer **2** exhibits only one absorption process in the investigated temperature and frequency ranges, which is ascribed to the dynamics of the main chain.

4. DSC investigations

Results from standard DSC and temperature modulated DSC (TMDSC) for polymers **2** and **1** are shown in figures 4 and 5, respectively. For polymer **1**, the clearing and glass transition temperatures were found to be 396 and 290 K, respectively. Both were very easily detectable as maxima in the c_p'' vs T curve. By

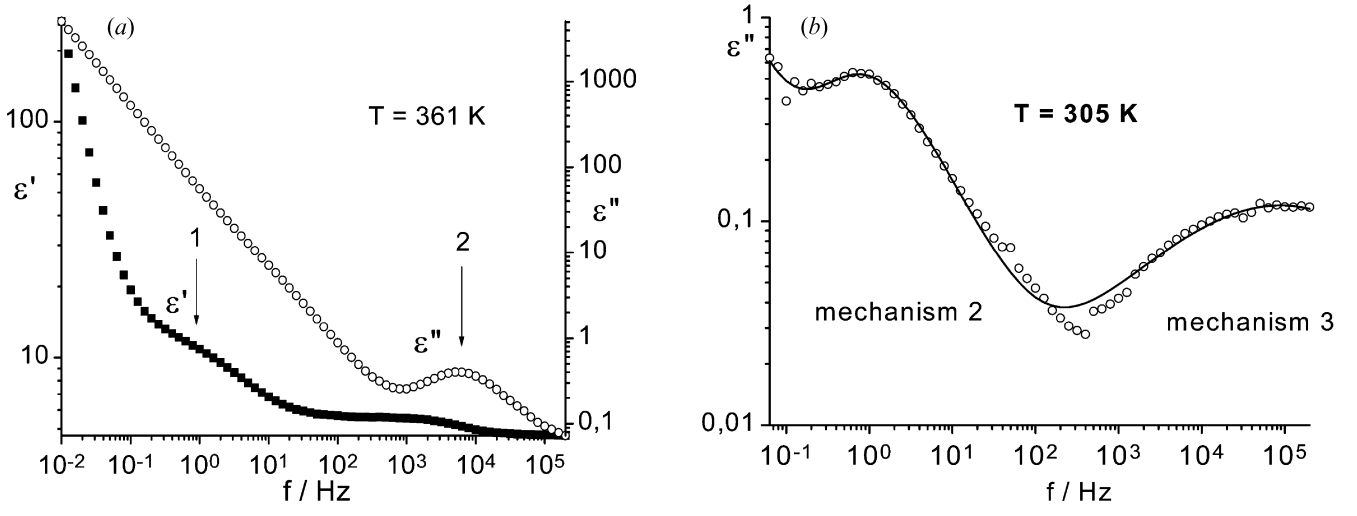

Figure 1. Variation of dielectric functions with frequency at two temperature. (*a*) Mechanisms 1 and 2, (*b*) Mechanism 3; measured values minus the data caused by the standing wave, fitted to equation (1). Due to the small absorption intensity the data were taken only up to 2 MHz. At $T<288$ K the experimental data could not be well fitted because of the stronger scattering and overlapping with mechanism 2.

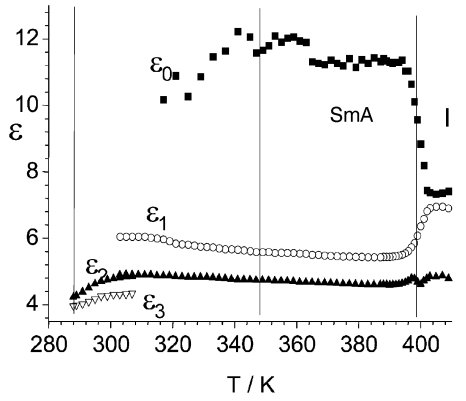

Figure 2. Limits of the dielectric functions and relaxation times of polymer **1**. Vertical lines indicate phase transition temperatures.

comparison with the dielectric relaxation times in figure 3 the glass transition at 290 K can be related to the cooperative reorganization of the main chains characterized by the time constant τ_2. In order to avoid confusion between the dielectric relaxation mechanism discussed previously and the calorimetric active processes, the same numbers are assigned to the same relaxation processes. This assignment is based on the data shown in figure 3. Therefore, the first glass process seen at 290 K is named T_g^2.

An additional peak in the $c_p(T)$ curve observed at 348 K is not seen in the dielectric measurements. This peak is relatively weak and shows no frequency dependence or relaxation response. Therefore it cannot be attributed to a glass transition mechanism. This calorimetric effect may be caused by a SmA/SmC transition, an interpretation which is supported by the

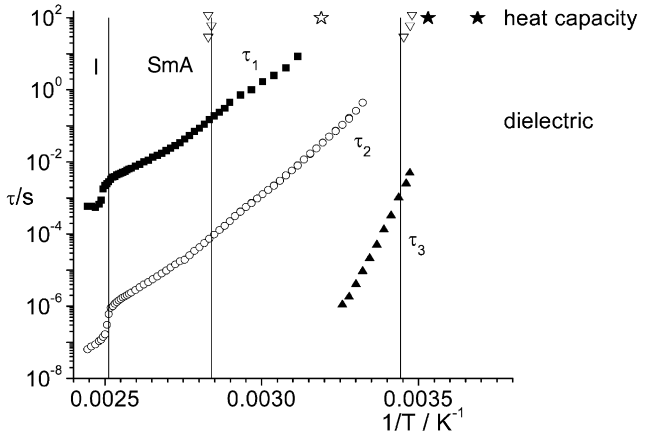

Figure 3. Dielectric relaxation times and maximum of c_p'' from TMDSC seen for three different periods (t_p=30 s, 60 s (figure 5) and 120 s) (∇). The stars represent results from standard DSC and enthalpy relaxation measurements, as given in figures 6 (*a*) and 6 (*b*) (τ=100 s).

decrease of ε_0 due to the tilt of the side groups within the layers as seen in figure 2. A confirmation of this transition by X-ray measurements failed because no orientation of the sample could be obtained.

Repeated cooling and heating runs between 233 and 413 K enhanced the resolution of two additional small anomalies in the DSC traces seen in figures 6(a) and (c), namely the small steps at 271 and 322 K, respectively. To obtain a better resolution, enthalpy relaxation experiments were performed which usually show the highest response for the annealing temperature $T_a \approx T_g$[11]. Using this method we found two temperature regions with two local maxima for the response as shown in figure 6 (*b*). These maxima can be interpreted as two different glass temperatures, T_g^2 discussed already and T_g^3. T_g^3 seen at 271 K corresponds well to τ_3 from dielectric measurements as shown in figure 3; therefore this second glass process can be assigned to the freezing-in of the dynamics of the side groups. The small step in the c_p curve at 322 K is in good agreement with the τ_1 process, the reorientation of the side group about the main chain (δ-relaxation). A confirmation of this result comes from a small but reproducible change in c_p in the order of magnitude of 0.005 J g^{-1} K^{-1} detected for long annealing times (t_a>1 h) in the temperature range from 313–325 K.

According to figure 5, sample **2** exhibits only one glass transition temperature at T_g=206 K. There is an indication of a weak calorimetric effect at 250 K, seen in both conventional DSC and in TMDSC as a small broad peak in the real as well as in the imaginary part of $\mathbf{c_p}$*. This effect may be caused by the crystallization or

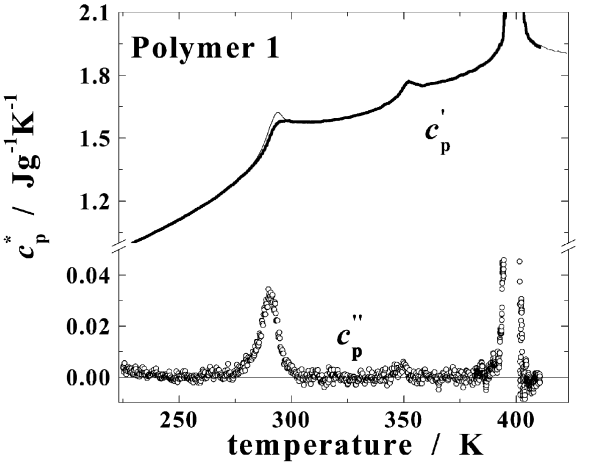

Figure 4. Standard DSC heating scan for polymer **1** at 10 K min^{-1} after cooling at 10 K min^{-1} (thin line), real part c_p' (thick line) and imaginary part c_p'' (°) from TMDSC with period t_p=60 s, temperature amplitude T_A=0.4 K and underlying heating rate q=2 K min^{-1}. The measurements are from the first and second heating run as an overview.

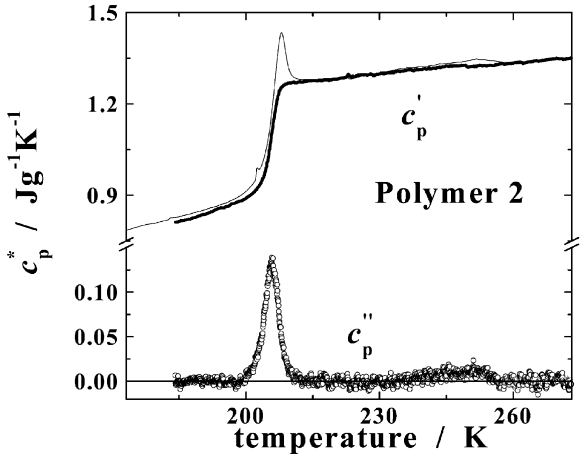

Figure 5. As figure 4 but for polymer **2**, with the following TMDSC parameters: period t_p=60 s, temperature amplitude T_A=0.3 K and underlying cooling rate q=0.5 K min^{-1}.

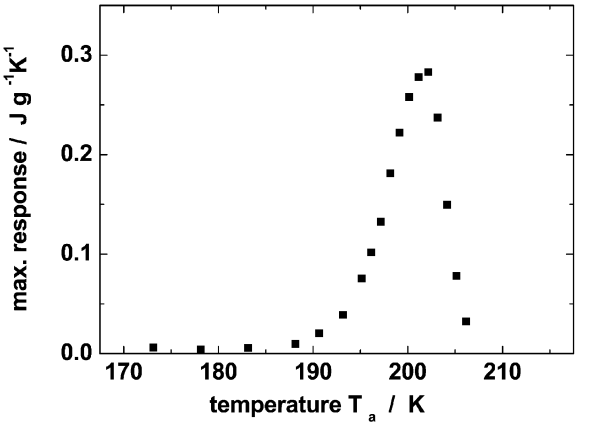

Figure 7. Enthalpy relaxation measurements on polymer **2**. Measurements were made in an analogous manner to those on polymer **1**, shown in figure 6 (*b*).

melting of side chains in the cooling or heating run, respectively, or simply by small impurities. For comparison, enthalpy relaxation measurements of sample **2** were also made. The experimental points and the fitted curve are given in figure 7 and can be compared with the results on sample **1** given in figure 6 (*b*). The difference between the figures is that sample **2** does not show the second glass relaxation at lower temperatures.

5. NMR measurements

To obtain a better understanding of the nature of the third dielectric relaxation process, dynamic MAS–NMR experiments were performed. The MAS spectrum

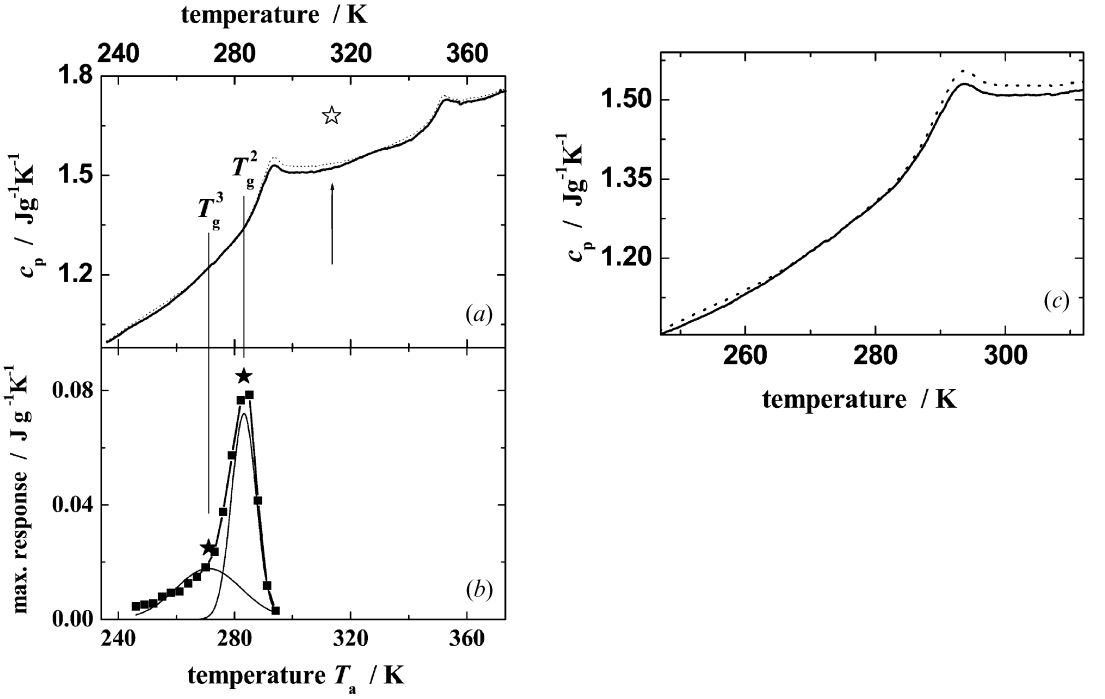

Figure 6. (*a*) First DSC heating run after cooling (dotted line) and DSC heating run after several repetitions (solid line) for polymer **1**. The numbers are related to the corresponding relaxation times τ_2 and τ_3, respectively (figure 4). The steps at T_g^3 and at 322 K (open star) are not seen in the first heating run. (*b*) Response from enthalpy relaxation experiments with an annealing time of 10 min for a set of temperature T_a. The solid stars are the maximum from a Gaussian fit and correspond to T_g^2 and T_g^3. (*c*) Enlargement of the glass transitions from (*a*).

of a $I=1/2$ nucleus (like ^{13}C) in a rigid solid rotating with a frequency ν_R consists of spinning side bands (ssb), centred around the chemical shift and separated by ν_R. Spinning side bands of observable intensity appear in the spectral range that is approximately equal to the span of the powder pattern due to the anisotropy of the chemical shift (CSA), $\Delta\sigma$ [18]. The ssb are the representation of the periodicity of the MAS time-domain signal which is imposed by the macroscopic rotation of the sample. The occurrence of dynamic processes with correlation times τ_c approximately equal to $1/\nu_R = T_R$ disturb the periodicity of the MAS-NMR signal, leading to the so-called dynamic broadening of the ssb [18–19]. Coming from a regime where $\tau_c > T_R$ (low temperatures), the line widths of the individual ssb start to increase and reach a maximum value for $\tau_c \cong T_R$, followed by a decrease of the line width at shorter τ_c (high temperatures). The maximum line width depends strongly on the ratio between the width of the CSA, $\Delta\sigma$, and the rotation frequency ν_R: the larger the ratio $\nu_R/\Delta\sigma$ (the faster the spinning), the smaller is the maximum of the dynamic line broadening. A value of $\nu_R/\Delta\sigma$ approximately equal to 1/4 appears to be a good compromise between a feasible signal to noise ratio, spectral resolution, and a reasonable maximum dynamic broadening.

The experiments were performed using a 7 mm Varian VT-CPMAS probe with a Varian Inova spectrometer operating at a resonance frequency of 100 MHz for ^{13}C and 149 MHz for ^{119}Sn. Cross-polarization (CP)

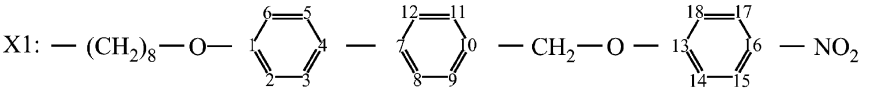

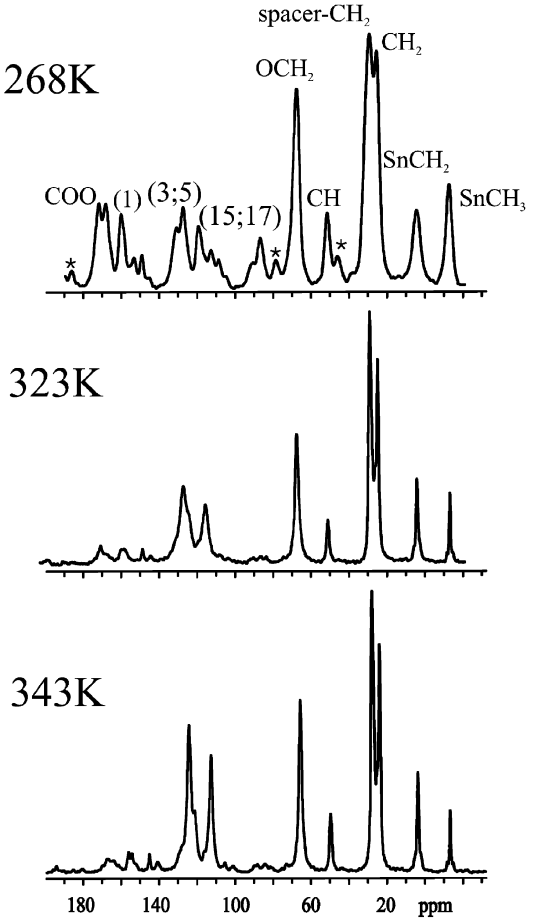

Figure 8. ^{13}C MAS spectra of polymer **2** for selected temperatures, and the assignment of the lines. The spectra were recorded at a spinning rate of 4 kHz with a recycle time of 3 s.

with a contact time of 0.5 ms was applied. The ^{13}C MAS spectra obtained are shown in figure 8 for various temperatures, together with the chemical structure of the sample. At lower temperatures (268 K) in general the lines are relatively well resolved. Those belonging to COO (27, 18), aromatic *para* (1,43) and -*ortho* carbons (3, 5, 21, 25, 41, 42, 44, 45) have a large intensity. On increasing the temperature to room temperature the aliphatic resonances (−20–+30 ppm) tend to narrow while these of the aromatic lines broaden. On further increase of the temperature towards 348 K (the second step observed in the calorimetric experiments) the line widths of all resonances decrease.

By plotting the full width of the line at half-height for different temperatures the existence of a dynamic process was detected. The results presented in figure 9 show the typical dynamic-MAS behaviour of the line width, as described already except for the step-like feature around 250 K, for lines belonging to the aromatic-*ortho* carbons. One can see the broadening effect of the lines belonging to the aromatic *ortho*-positions at temperatures ranging from 280 to 320 K (figure 9). Since no broadening is seen for the *para*-carbons, this broadening was identified with the 180° flip of the aromatic ring around the axis of the side chains. The correlation time of this process was estimated from the MAS-spinning rate to be $\tau_c \approx (2\pi \times 4\,\text{kHz})^{-1} = 40\,\mu\text{s}$ at 298 K, a value which agrees well with the third relaxation process trace of the dielectric measurements shown in figure 3. Investigations regarding the dynamic of other lines (main chain, spacer, etc.) showed no evidence of motion in the corresponding temperature–correlation time window. NMR-MAS experiments using ^{119}Sn as the probe nucleus were performed at a spinning rate of 4 kHz for several temperatures in the region of interest (250–350 K), but no evidence of motion was found. This emphasizes that the process detected by dynamic MAS-NMR is due solely to the rotation of the side chains around their long axes.

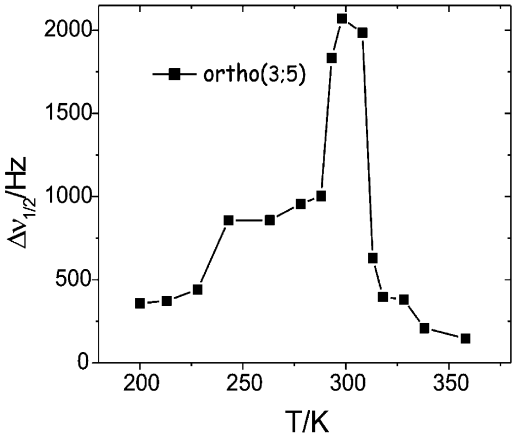

Figure 9. Plot of the line-width at full half-height versus temperature for one of the carbons *in* the aromatic *ortho*-positions, revealing flip around the long axis of the side chains.

6. Conclusion

All experimental results of the mesomorphic compound are summarized in figure 3. Two glass transitions related to the dynamics of different parts of the polymeric molecule were found. The higher glass temperature T_g^2 is related to motion within the main chain. This could be clearly detected by both methods applied, dielectric and TMDSC, in both samples. The freezing-in process for the reorientation of side groups about their long axes was observed only in the liquid crystalline polymer. The nature of this motion was confirmed by NMR measurements. We have to note that this process was also found by enthalpy relaxation experiments as T_g^3. Thus, the data support the model of phase separation in the investigated tin-containing polymer **1**; it is probably also valid for other liquid crystalline polymers. The dielectric active reorientation of the side group about the main chain also shows a weak calorimetric response. In the light of the new results the measurements published proviously [7] must be reinvestigated.

Acknowledgements

The authors are indebted to the DFG (SFB 418) for financial support and Prof. E. Donth and Dr S. Diele for helpful discussions.

References

[1] C. Tschierske. *J. mater. Chem.*, **6**, 1485 (1998).
[2] S. Westphal, S. Diele, A. Mädicke, F. Kuschel, U. Schem, K. Rühlmann, B. Hisgen, H. Ringsdorf. *Makromol. Chem., rapid Commun.*, **9**, 489 (1988).
[3] G. Mao, C. Oberer. *Handbook of Liquid Crystals*, D. Demus, J. Goodby, G.W. Gray, H.W. Spiess, V. Vill (Eds), Chap. III, Wiley-VCH, Weinheim (1998).
[4] Z. Roslaniec. In *Block Copolymers*, F.J.B. Calleja, Z. Roslaniec (Eds), Chap. 17, Marcel Dekker, New York (2000).
[5] S. Poser, H. Fischer, M. Arnold. In *Progress in Polymer Science*, O. Vogl, G .D. Jaycox, J.C. Vogl (Eds), Vol. 23, pp. 1337–1379, Elsevier Science (1998).
[6] Z. Roslaniec. In *Block Copolymers*, F.J.B. Calleja, Z. Roslaniec (Eds), Chap. 12, Marcel Dekker, New York (2000); Hamley. *The Physics of Block Copolymers* (Oxford University Press) (1998); G. H. Fredrickson, F. S. Bates. *Ann. Rev. mater. Sci.*, **26**, 501 (1996).

[7] U. Emmerling, J. Lindau, S. Diele, J. Werner, H. Kresse. *Liq. Cryst.*, **27**, 1069 (2000).
[8] V.P. Shibaev. *LC Polymers*, A. Plate (Ed.), pp. 193–249, Plenum Press, New York (1993).
[9] S. Diele, S. Oelsner, F. Kuschel, B. Hisgen, H. Ringsdorf. *Mol. Cryst. liq. Cryst.*, **155**, 399 (1988).
[10] F. Kuschel, A. Mädicke, S. Diele, H. Utschik, B. Hisgen, H. Ringsdorf. *Pol. Bul.*, **23**, 373 (1990).
[11] E. Hempel, M. Beiner, H. Huth, E. Donth. *Thermochimi. Acta*, **391**, 219 (2002).
[12] M. Beiner, K. Schröter, E. Hempel, S. Reissig, E. Donth. *Macromolecules*, **32**, 6278 (1999).
[13] M. Beiner, O. Kabisch, S. Reichl, H. Huth. *J. non-cryst. Solids*, **6658**, 307 (2002).
[14] E. Donth. *J. non-cryst. Solids*, **53**, 325 (1982), E. Donth. *The Glass Transition, Relaxation Dynamics in Liquids and Disordered Materials*, Berlin: Springer (2001).
[15] H. Kresse, R. Talroze. *Macromol. Chem. rapid. Commun.*, **2**, 369 (1981).
[16] R. Zentel, G. Strobl, H. Ringsdorf. *Recent Advances in Liquid Crystal line Polymers*, L.L. Chapoy (Ed.),(Elsevier Applied Sciences) (1985).
[17] H. Kresse, V.P. Shibaev. *Z. phys. Chem.*, **264**, 161 (1983).
[18] D. Reichert, E. Hempel, G. Zimmermann, H. Schneider, H. Luz. *J. solid state NMR*, **18**, 17 (2000).
[19] D. Suwelack, W.P. Rothwell, J.S. Waugh. *J. chem. Phys.*, **73**, 2559 (1980).